Adaptive Event-Triggered Control for Nonlinear Systems with Asymmetric State Constraints: A Prescribed-Time Approach

Ziwei Wang, *Member, IEEE*, Hak-Keung Lam, *Fellow, IEEE*, Yao Guo, *Member, IEEE*, Bo Xiao, *Member, IEEE*, Yanan Li, *Senior Member, IEEE*, Xiaojie Su, *Senior Member, IEEE*, Eric M. Yeatman, *Fellow, IEEE*, and Etienne Burdet, *Member, IEEE*

***Abstract*— Finite/Fixed-time control yields a promising tool to optimize a system's settling time, but lacks the ability to separately define the settling time and the convergence domain (known as *practically prescribed-time stability*, PPTS). We provide a sufficient condition for PPTS based on a new piecewise exponential function, which decouples the settling time and convergence domain into separately user-defined parameters. We propose an adaptive event-triggered prescribed-time control scheme for nonlinear systems with asymmetric output constraints, using an exponential-type barrier Lyapunov function. We show that this PPTS control scheme can guarantee tracking error convergence performance, while restricting the output state according to the prescribed asymmetric constraints. Compared with traditional finite/fixed-time control, the proposed methodology yields separately user-defined settling time and convergence domain without the prior information on disturbance. Moreover, asymmetric state constraints can be handled in the control structure through bias state transformation, which offers an intuitive analysis technique for general constraint issues. Simulation and experiment results on a heterogeneous teleoperation system demonstrate the merits of the proposed control scheme.**

***Index Terms*— Nonlinear systems, prescribed-time stability, state constraint, event-triggered control.**

I. Introduction

Stability is one important aspect in control design of nonlinear multi-input multi-output (MIMO) systems, where asymptotic stability plays a major role from theory to application. The system trajectory under asymptotically stable controllers reaches equilibrium when the settling time tends to infinity, whereas finite-time control provides a parameterised settling time for controller design. In [1], [2], a classic Lyapunov-based finite-time stability criterion revealed that the upper bound of the settling time can be regulated through initial values and control parameters. Subsequently, various finite-time concepts [3]–[6] were developed to obtain a more accurate settling time estimate [7]–[10]. However, the above estimate results depend on the initial value, leading to estimation conservatism in the presence of sensor noise and partial observations. To address this problem, fixed-time stability [11] was developed to relax the need for prior knowledge on initial conditions, and to give a uniform settling time constrained only by control parameters, which thus facilitates state-feedback control [12]–[14] and observer design [15]. Although the aforementioned works realized fixed-time stability to some extent, one would like to select a settling time arbitrarily according to task requirements rather than constrained by the control parameters. Furthermore, the aforementioned "finite/fixed time" refers to the upper bound of the setting time instead of the actual one which we would like to attain.

Therefore, partial performance metrics cannot be user-defined when applying the traditional finite/fixed-time controller. Settling time was used in [16], [17] as an explicit parameter rather than the corresponding control metric, thereby facilitating a new paradigm switch from finite-time stability to prescribed-time stability (PTS). The time transformation technique was proposed for PTS analysis and control synthesis, which effectively mapped the time domain to the user-defined range [18], [19]. However, few works investigated the user-defined properties for settling time and convergence domain simultaneously, i.e., practically prescribed-time stability (PPTS). In [20], [21], a time-varying fractional function based control method was proposed to achieve a user-defined settling time for high-order nonlinear systems. However, the convergent accuracy was determined by the upper bound of disturbances. PTS was realized for strict-feedback-like systems in the framework of state-feedback and output-feedback control [22], [23], but lacked the ability for a user to define the convergence behaviour of the system, independent of the settling time. Moreover, actuators commanded with the PTS principle behave on the basis of control period (sample time) at the cost of increased communication burden and excessive energy consumption. In contrast to time-based approaches, event-triggered mechanisms create a new paradigm for control systems subject to limited data transmission, which determines the state update or controller implementation according to specialized event conditions [24]. It is shown in [25] that introducing a dynamic event-triggered mechanism offers higher design flexibility to exclude Zeno phenomenon. For instance, the adaptive event-triggered methods in [26]–[28] leverage the communication resources in the actuation channel, reducing the computational burden, though they only achieved asymmetric stability. Compared to continuous triggering, interval actuator triggering will inevitably weaken control performance, leading to a conflict between the number of triggers and stable behaviour. Although the PTS concept was successfully introduced in multiagent systems [29], the PPTS property has not been explored in existing event-triggered works. Ensuring the PPTS property under an event-triggered mechanism therefore remains a challenge.

In addition, the system states are inevitably subject to specific constraints according to physical limitations and motion requirements. As an example, if the end-effector of a space robot moves beyond the field of view of the hand-eye camera, the target will be lost, thereby leading to docking task failure. Therefore, the constraints imposed on the control system facilitate safe and smooth task execution. Since predetermined constraints are incorporated in stability analysis and control synthesis, barrier Lyapunov functions (BLF) become an effective approach to dealing with constraint control problems. As the associated state approaches a predetermined constraint, the BLF will tend to infinity thereby resulting in a large control input that regulates the system state within the constraint range. Log-

This work was supported in part by the European Commission Grant H2020 PH-CODING (FETOPEN 829186), CONBOTS (ICT 871803), and the U.K. EPSRC Grants EP/R026092/1, EP/P012779/1. (Corresponding author: Ziwei Wang and Etienne Burdet)

Ziwei Wang, Bo Xiao, Eric M. Yeatman, and Etienne Burdet are with Imperial College of Science, Technology and Medicine, SW7 2AZ, United Kingdom (e-mail: e.burdet@imperial.ac.uk).

Hak-Keung Lam is with the Department of Engineering, King's College London, Strand, London, WC2R 2LS, United Kingdom.

Yao Guo is with the Institute of Medical Robotics, Shanghai Jiao Tong University, Shanghai 200400, China.

Yanan Li is with the Department of Engineering and Design, University of Sussex, Brighton BN1 9RH, United Kingdom.

Xiaojie Su is with the School of Automation, Chongqing University, Chongqing 400044, China.

type [30] and tan-type [31] BLF were introduced to tackle output state constraints and applied to stochastic nonlinear systems [32]. Recently, we proposed a novel exponential-type BLF (EBLF) applied to state feedback [33], [34], which was beneficial to address nonlinear systems with symmetric state constraints. Several works [35]–[37] attempted to consider asymmetric state constraints using piecewise Lyapunov functions, but the time-derivative terms of a Lyapunov function may increase the control input, leading to increased energy use. In [12], upper and lower bound functions were integrated to a Lyapunov function, whereas the prescribed-time property was not considered.

Motivated by the above observations, we investigate the prescribed-time stabilization of nonlinear MIMO systems subject to asymmetric constraints. Parametric uncertainty, additive disturbance, and asymmetric output constraints can be addressed effectively in the proposed adaptive event-triggered control scheme, simultaneously guaranteeing the user-defined settling time and convergence domain.

The contributions of this paper are threefold:

(i) A new sufficient condition for PPTS is provided to ensure user-defined characteristics of settling time and convergence domain. These two metrics can be preset simultaneously, which addresses the limit caused by control parameter constraints and thus enables to decouple response speed and accuracy.

(ii) The EBLF technique is combined with back-stepping control to impose time-varying asymmetric output constraints, which transforms an asymmetric constraint into a symmetric one by bias state transformation. Different from approaches that deal with asymmetric constraints [30], [35]–[37], the proposed framework eliminates the need to determine the sign of the constraint state or its state transformation variables in real time.

(iii) In contrast to adaptive event-triggered methods employing the universal approximation theorem [26]–[28], the proposed control scheme can ensure the robustness against parametric uncertainty and additive disturbances while overcoming the contradiction between control accuracy and event-triggered mechanism. This allows convergence accuracy to be quantitatively calculated and artificially predetermined, without depending on disturbance upper bounds.

II. Preliminaries

We use the following notations: $\mathbb{Z}_+$ denotes the set of positive natural numbers. $\mathbb{R}_{\geq 0}$ stands for the set of non-negative real numbers. I_n denotes the identity matrix of dimension n. $\forall A \in \mathbb{R}^{n\times n}$, $\|A\|$ is the Frobenius norm. The superscript $(\cdot)^{(i)}$ represents the ith time-derivative. $\mathrm{diag}\{a_j\}$ and $\mathrm{col}\{a_j\}$ stand for the diagonal matrix and column vector with a_j as the jth entry, respectively.

Consider the following nonlinear system

$$\dot{x}(t) = f(x(t), t) \tag{1}$$

where $x(t) \in \mathbb{R}^n$ is the system state and $f : \mathbb{R}^n \times \mathbb{R}_{\geq 0} \to \mathbb{R}^n$ a continuous-differential function. The equilibrium of (1) is *practically prescribed-time stable* (PPTS) if $\|x(t)\| \leq \varepsilon$ for $t \geq t_0 + T$, where t_0 is the initial time, ε the convergence domain, and T the settling time which are defined by the user within an achievable range. $T_s \leq T < +\infty$, with T_s denoting the time consumed in the necessary data transmission and processing. Notice that the arbitrary setting of ε and T is emphasized in the concept of PPTS, i.e., ε and T are decoupled. In order to achieve PPTS, we introduce a time-varying piecewise function:

$$\varsigma(t) = \begin{cases} \exp[\alpha\,(t_T - t)] - 1, & t \in [t_0, t_T) \\ \exp[\alpha\,(t - t_T)], & t \in [t_T, +\infty) \end{cases} \tag{2}$$

where $t_T = t_0 + T$ and $\alpha \in (0, \ln(2)/T]$ is a tuning parameter.

Theorem 1: If there exists a positive-definite continuous-differential function $V(x(t), t) : \mathbb{R}^n \times \mathbb{R}_{\geq 0} \to \mathbb{R}_{\geq 0}$ and positive scalars a, b, c such that $a > \alpha$, $b > c$, and

$$\dot{V} \leq -\left(a + \frac{|\dot{\varsigma}|}{\varsigma}\right) V + \frac{b}{\varsigma} + c, \tag{3}$$

then the equilibrium of system (1) is PPTS and the system trajectory will enter the convergence domain $\Omega = \{x \,|V(x) \leq b/\alpha\}$ for $t \geq t_T$.

Proof. For $t \in [t_0, t_T)$, the time-derivative of V/ς is derived by integrating (3)

$$\frac{d}{dt}\left(\frac{V}{\varsigma}\right) \leq \frac{\dot{V}}{\varsigma} + \frac{|\dot{\varsigma}|}{\varsigma^2} V \leq -a\left(\frac{V}{\varsigma}\right) + \frac{b}{\varsigma^2} + \frac{c}{\varsigma}. \tag{4}$$

The uniformly ultimately bounded (UUB) stability can be guaranteed by applying the Lyapunov theorem [38]. Moreover, with the Comparison Theorem, integrating both sides of (4) yields

$$\begin{aligned} \frac{V(t)}{\varsigma(t)} \leq\ & \mathrm{e}^{-a(t-t_0)} \frac{V(t_0)}{\varsigma(t_0)} \\ & + \mathrm{e}^{-a(t-t_T)} \left[(c-b)(t_T - t) + \frac{b}{\alpha}\frac{\varsigma + 1}{\varsigma} - \frac{c-b}{\alpha}\ln\varsigma\right]. \end{aligned} \tag{5}$$

Note that $\alpha \in (0, \ln(2)/T]$ leads to $\ln(\varsigma) \leq 0$, which implies the monotonically decreasing property of $V(t)$ for $t \in [t_0, t_T)$. Since $\varsigma(t) \to 0$ at $t \to t_T$ and $\lim_{\varsigma\to 0} \varsigma\ln\varsigma = 0$, we have $V(t_T) = \lim\limits_{t\to t_T} V(t) \leq \frac{b}{\alpha}$. Therefore, the system trajectory approaches a certain region Ω when $t = t_T$. It is worth pointing out that the boundary of Ω only depends on the user-designed parameters rather than system dynamics. Thus, the convergence accuracy can be user-defined according to practical task requirements.

For $t \geq t_T$, substituting (2) into condition (3) leads to

$$\dot{V} \leq -(a + \alpha) V + 2b. \tag{6}$$

Furthermore, integrating both sides of (6), we have

$$\begin{aligned} V(t) &\leq \mathrm{e}^{-(a+\alpha)(t-t_T)} V(t_T) + \frac{2b}{a+\alpha}\left[1 - \mathrm{e}^{-(a+\alpha)(t-t_T)}\right] \\ &\leq \frac{b}{\alpha}\mathrm{e}^{-(a+\alpha)(t-t_T)} + \frac{2b}{a+\alpha}\left[1 - \mathrm{e}^{-(a+\alpha)(t-t_T)}\right] < \frac{b}{\alpha}. \end{aligned} \tag{7}$$

Therefore, the system trajectory will never leave Ω for $t \in (t_T, +\infty)$, which completes the proof.

Remark 1: Different from the UUB stability, the settling time in PPTS is not constrained by the initial range or ultimate bound. In addition, the ultimate bound does not depend on disturbances or system uncertainties. Different from traditional concepts of finite/fixed/prescribed-time stability, the settling time and accuracy are treated as independent parameters in PPTS.

Remark 2: Compared with the existing prescribed-time controllers [33], [34], we have carried out a more rigorous stability analysis of the transient-state process and quantitatively given the selection basis of corresponding parameters in this paper. α is adjusted according to a predetermined convergence time rather than a fixed empirical parameter. The scalar function (2) at $t > t_T$ is replaced by an exponential form so that the system trajectory will converge in an asymptotic form after the scheduled settling time. In this regard, we reveal the relationship among PPTS, asymptotic stability and UUB stability in the case $t > t_T$.

Remark 3: The following properties of the piecewise function (2) are instrumental for the implementation of PPTS in the period of $t \in [t_0, t_T)$: i) $\varsigma(t)$ is monotonically decreasing and constantly positive, ii) $\varsigma(t) \to 0$ i.f.f. $t \to t_T$, and iii) $\lim_{\varsigma\to 0} \varsigma\ln\varsigma = 0$. Therefore, $\mathcal{C}^\infty$ functions that fulfill these three properties can be

also used as (2). In terms of implementation, the right derivative of $\varsigma(t)$ is defined as $\dot{\varsigma}(t)$ at $t = t_T$. Three parameters (α, a, and b) also play an essential role in the realization of PPTS. Given the settling time and accuracy requirements, larger α and a (or smaller b) within the admissible range facilitate accuracy improvement, but may lead to excessive control gain. Hence, there is a trade-off for parameter regulation according to the practical demand on physically available resources (communication bandwidth, maximum actuation torque, etc.).

III. Main Result

Consider a class of nonlinear MIMO systems with parametric uncertainty and additive disturbance

$$\begin{cases} \dot{x}_i(t) = A_i(\bar{x}_i(t), t)x_{i+1}(t) + B_i^{\mathrm{T}}(t)f_i(t) + h_i(\bar{x}_i(t), t), \\ i = 1, 2, ..., n-1, \\ \dot{x}_n(t) = A_n(\bar{x}_n(t), t)u(t) + B_n^{\mathrm{T}}(t)f_n(t) + h_n(\bar{x}_n(t), t), \\ y(t) = x_1(t), \end{cases} \tag{8}$$

where $x_i(t) \in \mathbb{R}^{n_i}$ is the state vector, $A_i(\bar{x}_i(t), t) \in \mathbb{R}^{n_i \times n_i}$ the unknown gain function with $\bar{x}_i(t) = [x_1(t)^{\mathrm{T}}, ..., x_i(t)^{\mathrm{T}}]^{\mathrm{T}}$, $i = 1, 2, ..., n$, $y(t)$ the system output, $B_i(t) \in \mathbb{R}^{p_i \times n_i}$ the unknown parametric function while $f_i(t) \in \mathbb{R}^{p_i}$ is a known nonlinear function, $h_i(\bar{x}_i(t), t)$ the unknown non-parametric disturbance, and $u(t) \in \mathbb{R}^{n_n}$ the control input. The following assumptions are needed for $i = 1, 2, ..., n$.

Assumption 1. There exist two constants $\underline{a}_i$ and $\bar{a}_i$ such that $0 < \underline{a}_i \leq \|A_i(\bar{x}_i(t), t)\| \leq \bar{a}_i$.

Assumption 2. $B_i(t)$ and $h_i(\bar{x}_i(t), t)$ are subject to $\|B_i(t)\| \leq \bar{b}_i$ and $\|h_i(\bar{x}_i(t), t)\| \leq \bar{h}_i \|\bar{x}_i(t)\|$, where $\bar{b}_i$ and $\bar{h}_i$ are unknown constants.

Remark 4: Since the associated functions above are composed of system states subject to measurement range, *Assumptions* 1-2 are rational in practical applications [39]. In addition, although gain functions $A_i(\bar{x}_i(t), t)$ and appended disturbances $h_i(\bar{x}_i(t), t)$ are state-dependent with constant upper bounds, they are only used in stability analysis rather than controller implementation or accuracy calculation.

In order to deal with the computational burden induced by frequent controller triggers, a dynamic mechanism is required to determine whether to send updated control input to the plant. Here we implement an event-triggered control scheme with a time-varying relative threshold [40] as follows:

$$u_j(t) = \tau_j(t_k), \forall t \in [t_k, t_{k+1}), k \in \mathbb{Z}_+ \tag{9}$$

$$t_{k+1} = \inf\{t > t_k | \left|\tau_j(t) - u_j(t)\right| \geq \beta_j \left|u_j(t)\right| + \gamma_j\} \tag{10}$$

where β_j and γ_j are positive design parameters, t_k is the update time, and $u_j(t)$, $\tau_j(t_k)$ are the jth element of $u(t)$ and $\tau(t_k)$, respectively. Once the mechanism (10) is triggered, the control input $u_j(t)$ will be updated by the intermediate virtual control law $\tau_j(t_{k+1})$. Thus, for $t \in [t_k, t_{k+1})$, $u_j(t)$ remains at $\tau_j(t)$ updated at the last moment such that

$$\left|\tau_j(t) - u_j(t)\right| \leq \beta_j \left|u_j(t)\right| + \gamma_j, \tag{11}$$

which further indicates $u_j(t) = \frac{\tau_j(t)}{1+\varrho_{1j}(t)\beta_j} - \frac{\varrho_{2j}(t)\gamma_j}{1+\varrho_{1j}(t)\beta_j}$, where $\varrho_{1j}(t)$, $\varrho_{2j}(t) \in [-1, 1]$ are the time-varying threshold parameters. Given $\vartheta_1 = \mathrm{diag}\{1/1 + \varrho_{1j}(t)\beta_j\}$ and $\vartheta_2 = -\mathrm{col}\{\varrho_{2j}(t)\gamma_j/1 + \varrho_{1j}(t)\beta_j\}$, a more compact form can be deduced as

$$u(t) = \vartheta_1 \tau(t) + \vartheta_2, \tag{12}$$

which also implies the boundedness of ϑ_1 and ϑ_2, namely there exist positive scalars $\underline{\vartheta}_1$, $\bar{\vartheta}_1$, $\underline{\vartheta}_2$, and $\bar{\vartheta}_2$ such that $\|\vartheta_1\| \in [\underline{\vartheta}_1, \bar{\vartheta}_1]$ and $\|\vartheta_2\| \in [\underline{\vartheta}_2, \bar{\vartheta}_2]$.

A. Controller Design

With the desired state denoted by $x_{id}(t) \in \mathbb{R}^{n_i}$, the tracking error is represented by $e_i(t) = x_i(t) - x_{id}(t)$. The control objective can be stated as follows. For the nonlinear MIMO system (8), design the event-triggered control scheme to guarantee the PPTS as well as asymmetric constraint performance of the tracking error. To this end, we utilize the back-stepping approach to conduct the overall stability design and control synthesis. To what follows, the arguments will be omitted without specific notes to avoid the ambiguity, e.g. $e_i \equiv e_i(t)$.

Step 1. Consider the state transformation $z_1 = e_1 + \Delta k_c$ and $z_2 = x_2 - \bar{v}_1$, where Δk_c is the bias constraint function and $\bar{v}_1$ is the auxiliary stabilizing function to be designed later. Then consider the exponential-type BLF (EBLF)

$$V_E = \frac{1}{2}k_c^2\left[\exp(k_c \circ z_1) - 1\right] \tag{13}$$

where $k_c \in \mathbb{R}_+$ is a C^∞ prescribed constraint function, $k_c(0) > \|z_1(0)\|$, and $k_c \circ z_1 = z_1^{\mathrm{T}} z_1/(k_c^2 - z_1^{\mathrm{T}} z_1)$. In general, the constraint function is set to limit state errors. Thus, a monotonically decreasing function that eventually tends to zero is chosen as constraint function. Then

$$\begin{aligned} \dot{V}_E &= \dot{k}_c k_c \big(\exp(k_c \circ z_1) - 1\big) + \exp(k_c \circ z_1)\frac{z_1^{\mathrm{T}}\dot{z}_1 k_c^4 - z_1^{\mathrm{T}} z_1 \dot{k}_c k_c^3}{(k_c^2 - z_1^{\mathrm{T}} z_1)^2} \\ &\leq -\dot{k}_c k_c - \frac{\dot{k}_c}{k_c}\xi_1 z_1^{\mathrm{T}} z_1 + \xi_1 z_1^{\mathrm{T}} \dot{z}_1 \end{aligned} \tag{14}$$

where $\xi_1 = k_c^4 \frac{\exp(k_c \circ z_1)}{(k_c^2 - z_1^{\mathrm{T}} z_1)^2}$. Recalling $z_1 = e_1 + \Delta k_c$, the dynamics of z_1 follows $\dot{z}_1 = A_1(z_2 + \bar{v}_1) + B_1^{\mathrm{T}} f_1 + h_1 - \dot{x}_{1d} + \Delta \dot{k}_c$. Then

$$\begin{aligned} \dot{V}_E \leq\ & \mu_c k_c^2 + \mu_c \xi_1 z_1^{\mathrm{T}} z_1 + \xi_1 z_1^{\mathrm{T}} A_1 z_2 \\ & + \xi_1 z_1^{\mathrm{T}}(A_1 \bar{v}_1 + B_1^{\mathrm{T}} f_1 + h_1 - \dot{x}_{1d} + \Delta \dot{k}_c) \end{aligned} \tag{15}$$

where $\mu_c = \sqrt{(\dot{k}_c/k_c)^2 + \epsilon_1}$ and $\epsilon_1 > 0$ is constant. Note that the following inequalities hold in (15)

$$z_1^{\mathrm{T}} B_1^{\mathrm{T}} f_1 \leq \|z_1\| \bar{b}_1 \|f_1\| \leq \epsilon_1 \bar{b}_1 + \bar{b}_1 \frac{z_1^{\mathrm{T}} z_1 f_1^{\mathrm{T}} f_1}{\sqrt{z_1^{\mathrm{T}} z_1 f_1^{\mathrm{T}} f_1 + \epsilon_1^2}}, \tag{16}$$

$$z_1^{\mathrm{T}} h_1 \leq \|z_1\| \bar{h}_1 \|x_1\| \leq \epsilon_1 \bar{h}_1 + \bar{h}_1 \frac{z_1^{\mathrm{T}} z_1 x_1^{\mathrm{T}} x_1}{\sqrt{z_1^{\mathrm{T}} z_1 x_1^{\mathrm{T}} x_1 + \epsilon_1^2}}. \tag{17}$$

Setting $\theta_1 \equiv [\bar{b}_1 I_n, \bar{h}_1 I_n]$, $\psi_1 \equiv [\frac{z_1 f_1^{\mathrm{T}} f_1}{\sqrt{z_1^{\mathrm{T}} z_1 f_1^{\mathrm{T}} f_1 + \epsilon_1^2}}; \frac{z_1 x_1^{\mathrm{T}} x_1}{\sqrt{z_1^{\mathrm{T}} z_1 x_1^{\mathrm{T}} x_1 + \epsilon_1^2}}]$, we conclude from (15) that

$$\begin{aligned} \dot{V}_E \leq\ & \mu_c k_c^2 + \mu_c \xi_1 z_1^{\mathrm{T}} z_1 + \xi_1 z_1^{\mathrm{T}} A_1 z_2 + \xi_1 z_1^{\mathrm{T}}(A_1 \bar{v}_1 - \dot{x}_{1d} \\ & + \Delta \dot{k}_c) + \xi_1 z_1^{\mathrm{T}} \theta_1 \psi_1 + \xi_1 \epsilon_1 (\bar{b}_1 + \bar{h}_1). \end{aligned} \tag{18}$$

Designing the auxiliary stabilizing function $\bar{v}_1$ as

$$\bar{v}_1 = -\frac{\hat{a}_1^2 v_1^{\mathrm{T}} v_1 z_1}{\sqrt{\hat{a}_1^2 v_1^{\mathrm{T}} v_1 z_1^{\mathrm{T}} z_1 + \epsilon_1^2}}, \tag{19}$$

$$\begin{aligned} v_1 =\ & \mu_c z_1 - \dot{x}_{1d} + \Delta \dot{k}_c + \hat{\theta}_1 \psi_1 - \left(\frac{b}{\varsigma} - \rho^2\right)\frac{z_1}{\xi_1 z_1^{\mathrm{T}} z_1} \\ & + \rho \frac{(k_c^2 - z_1^{\mathrm{T}} z_1)^2}{2k_c^2 z_1^{\mathrm{T}} z_1} z_1 + \frac{\xi_1 z_1}{2 z_1^{\mathrm{T}} z_1}, \end{aligned} \tag{20}$$

This article has been accepted for publication in IEEE Transactions on Automatic Control. This is the author's version which has not been fully edited and content may change prior to final publication. Citation information: DOI 10.1109/TAC.2022.3194880

where $a_1 = 1/\underline{a}_1$ and $\rho = \left(a + \frac{|\dot{\varsigma}|}{\varsigma}\right)$. $\hat{a}_1$ and $\hat{\theta}_1$ are the estimation of a_1 and θ_1, which are updated by

$$\dot{\hat{a}}_1 = \sigma_{a1}\xi_1 z_1^{\mathrm{T}}\upsilon_1 - \rho\hat{a}_1; \quad \dot{\hat{\theta}}_1 = \sigma_{\theta 1}\xi_1 z_1\psi_1^{\mathrm{T}} - \rho\hat{\theta}_1; \tag{21}$$

with σ_{a1} and $\sigma_{\theta 1}$ being positive scalars. Hence, combining (18) and (19) yields

$$z_1^{\mathrm{T}}A_1\bar{\upsilon}_1 \leq -\underline{a}_1\frac{\hat{a}_1^2\upsilon_1^{\mathrm{T}}\upsilon_1 z_1^{\mathrm{T}}z_1}{\sqrt{\hat{a}_1^2\upsilon_1^{\mathrm{T}}\upsilon_1 z_1^{\mathrm{T}}z_1 + \epsilon_1^2}} \leq \epsilon_1\underline{a}_1 - \underline{a}_1\hat{a}_1 z_1^{\mathrm{T}}\upsilon_1. \tag{22}$$

Consider the Lyapunov function candidate $V_1 = V_E + \frac{\underline{a}_1}{2\sigma_{a1}}\tilde{a}_1^2 + \frac{1}{2\sigma_{\theta 1}}\mathrm{tr}\big(\tilde{\theta}_1^{\mathrm{T}}\tilde{\theta}_1\big)$, where $\mathrm{tr}(\cdot)$ is the trace of corresponding matrix, $\tilde{a}_1 = \hat{a}_1 - a_1$ and $\tilde{\theta}_1 = \hat{\theta}_1 - \theta_1$. Using (19)-(22), the time-derivative of V_1 can be calculated as

$$\begin{aligned}\dot{V}_1 \leq\ & \mu_c k_c^2 + \mu_c\xi_1 z_1^{\mathrm{T}}z_1 + \xi_1 z_1^{\mathrm{T}}A_1 z_2 - \xi_1 z_1^{\mathrm{T}}\upsilon_1 \\ & + \xi_1 z_1^{\mathrm{T}}(-\dot{x}_{1d} + \Delta\dot{k}_c) + \xi_1 z_1^{\mathrm{T}}\theta_1\psi_1 + \mathrm{tr}\big(\tilde{\theta}_1^{\mathrm{T}}\xi_1 z_1\psi_1^{\mathrm{T}}\big) \\ & + \xi_1\epsilon_1(\bar{b}_1 + \bar{h}_1 + \underline{a}_1) - \frac{\underline{a}_1\rho}{\sigma_{a1}}\tilde{a}_1\hat{a}_1 - \frac{\rho}{\sigma_{\theta 1}}\mathrm{tr}\big(\tilde{\theta}_1^{\mathrm{T}}\hat{\theta}_1\big).\end{aligned} \tag{23}$$

The following inequalities hold in the last two terms of (23)

$$\begin{aligned}-\frac{\underline{a}_1\rho}{\sigma_{a1}}\tilde{a}_1\hat{a}_1 &= -\frac{\underline{a}_1\rho}{\sigma_{a1}}\tilde{a}_1^2 - \frac{\underline{a}_1\rho}{\sigma_{a1}}\tilde{a}_1 a_1 \\ &\leq -\frac{\underline{a}_1\rho}{2\sigma_{a1}}\tilde{a}_1^2 + \frac{1}{2}\rho^2 + \frac{a_1^2}{8\sigma_{a1}^2},\end{aligned} \tag{24}$$

$$-\frac{\rho}{\sigma_{\theta 1}}\mathrm{tr}\big(\tilde{\theta}_1^{\mathrm{T}}\hat{\theta}_1\big) \leq -\frac{\rho}{2\sigma_{\theta 1}}\mathrm{tr}\big(\tilde{\theta}_1^{\mathrm{T}}\tilde{\theta}_1\big) + \frac{1}{2}\rho^2 + \frac{\mathrm{tr}\big(\theta_1^{\mathrm{T}}\theta_1\big)^2}{8\sigma_{\theta 1}^2}. \tag{25}$$

Therefore, we have a more simplified form of $\dot{V}_1$ by substituting (20) and the above inequalities into (23)

$$\dot{V}_1 \leq \xi_1 z_1^{\mathrm{T}}A_1 z_2 - \rho V_1 + \frac{b}{\varsigma} + c_1 \tag{26}$$

where $c_1 = \mu_c k_c^2 + \frac{\epsilon_1^2}{2}(\bar{b}_1 + \bar{h}_1 + \underline{a}_1)^2 + \frac{a_1^2}{8\sigma_{a1}^2} + \frac{\mathrm{tr}\big(\theta_1^{\mathrm{T}}\theta_1\big)^2}{8\sigma_{\theta 1}^2}$. It can be concluded from (26) that the PPTS convergence of z_1 can be guaranteed if z_2 is stabilized.

Step k ($2 \leq k \leq n-1$). Define the state transition $z_k = x_k - \bar{\upsilon}_{k-1}$, in which $\bar{\upsilon}_{k-1}$ is the auxiliary stabilizing function. Introducing the Lyapunov function candidate: $V_k = V_{k-1} + \frac{1}{2}z_k^{\mathrm{T}}z_k + \frac{a_k}{2\sigma_{ak}}\tilde{a}_k^2 + \frac{1}{2\sigma_{\theta k}}\mathrm{tr}\big(\tilde{\theta}_k^{\mathrm{T}}\tilde{\theta}_k\big)$, where σ_{ak} and $\sigma_{\theta k}$ are positive scalars, $\tilde{a}_k = \hat{a}_k - a_k$, $\tilde{\theta}_k = \hat{\theta}_k - \theta_k$, and $a_k = 1/\underline{a}_k$, while $\hat{a}_k$ and $\hat{\theta}_k$ will be defined later. Taking the time-derivative of V_k and using inequalities similar to (16)-(17) yield

$$\begin{aligned}\dot{V}_k \leq\ & \dot{V}_{k-1} + z_k^{\mathrm{T}}A_k(z_{k+1} + \bar{\upsilon}_k) + \epsilon_k(\bar{b}_k + \bar{h}_k) \\ & + z_k^{\mathrm{T}}z_k\left(\frac{\bar{b}_k f_k^{\mathrm{T}}f_k}{\sqrt{z_k^{\mathrm{T}}z_k f_k^{\mathrm{T}}f_k + \epsilon_k^2}} + \frac{\bar{h}_k\|\bar{x}_k\|^2}{\sqrt{z_k^{\mathrm{T}}z_k\|\bar{x}_k\|^2 + \epsilon_k^2}}\right) \\ & - z_k^{\mathrm{T}}\varpi_k - z_k^{\mathrm{T}}\Xi_k + \frac{\underline{a}_k}{\sigma_{ak}}\tilde{a}_k\dot{\hat{a}}_k + \frac{1}{\sigma_{\theta k}}\mathrm{tr}\big(\tilde{\theta}_k^{\mathrm{T}}\dot{\hat{\theta}}_k\big)\end{aligned} \tag{27}$$

where $\varpi_k = \sum_{j=1}^{k-1}\frac{\partial\bar{\upsilon}_{k-1}}{\partial x_1^{(j-1)}}x_{1d}^{(j)} + \frac{\partial\bar{\upsilon}_{k-1}}{\partial k_c^{(j-1)}}k_c^{(j)} + \frac{\partial\bar{\upsilon}_{k-1}}{\partial\hat{\theta}_j}\dot{\hat{\theta}}_j + \frac{\partial\bar{\upsilon}_{k-1}}{\partial\Delta k_c^{(j-1)}}\Delta k_c^{(j)} + \frac{\partial\bar{\upsilon}_{k-1}}{\partial\hat{a}_j}\dot{\hat{a}}_j$ and $\Xi_k \equiv \sum_{j=1}^{k-1}\frac{\partial\bar{\upsilon}_{k-1}}{\partial x_j}(A_j x_{j+1} + B_j^{\mathrm{T}}f_j + h_j)$. Based on Young's inequality, we have

$$\begin{aligned}z_k^{\mathrm{T}}\Xi_k \leq\ & \sum_{j=1}^{k-1}\frac{\bar{a}_j z_k^{\mathrm{T}}z_k\|\frac{\partial\bar{\upsilon}_{k-1}}{\partial x_j}\|^2\left\|x_{j+1}\right\|^2}{\sqrt{z_k^{\mathrm{T}}z_k\|\frac{\partial\bar{\upsilon}_{k-1}}{\partial x_j}\|^2\left\|x_{j+1}\right\|^2 + \epsilon_j^2}} + \epsilon_j\bar{a}_j \\ & + \frac{\bar{b}_j z_k^{\mathrm{T}}z_k\|\frac{\partial\bar{\upsilon}_{k-1}}{\partial x_j}\|^2 f_j^{\mathrm{T}}f_j}{\sqrt{z_k^{\mathrm{T}}z_k\|\frac{\partial\bar{\upsilon}_{k-1}}{\partial x_j}\|^2 f_j^{\mathrm{T}}f_j + \epsilon_j^2}} + \epsilon_j\bar{b}_j \\ & + \frac{\bar{h}_j z_k^{\mathrm{T}}z_k\|\frac{\partial\bar{\upsilon}_{k-1}}{\partial x_j}\|^2\left\|\bar{x}_j\right\|^2}{\sqrt{z_k^{\mathrm{T}}z_k\|\frac{\partial\bar{\upsilon}_{k-1}}{\partial x_j}\|^2\left\|\bar{x}_j\right\|^2 + \epsilon_j^2}} + \epsilon_j\bar{h}_j\end{aligned} \tag{28}$$

where $\epsilon_j > 0$ for $j = 1, 2, ..., n$. Hence, substituting (28) into (27), one can obtain

$$\begin{aligned}\dot{V}_k \leq\ & -\rho V_1 + z_k^{\mathrm{T}}A_k z_{k+1} + z_k^{\mathrm{T}}A_k\bar{\upsilon}_k + \sum_{j=1}^{k}\epsilon_j(\bar{b}_j + \bar{h}_j) \\ & + \sum_{j=1}^{k-1}2\epsilon_j\bar{a}_j + z_k^{\mathrm{T}}\theta_k\psi_k - z_k^{\mathrm{T}}\varpi_k - \sum_{j=2}^{k-1}\rho\bigg(\frac{1}{2}z_j^{\mathrm{T}}z_j + \frac{\underline{a}_j}{2\sigma_{aj}}\tilde{a}_j^2 \\ & \frac{1}{2\sigma_{\theta j}}\mathrm{tr}\big(\tilde{\theta}_j^{\mathrm{T}}\tilde{\theta}_j\big)\bigg) + \frac{\underline{a}_k}{\sigma_{ak}}\tilde{a}_k\dot{\hat{a}}_k + \frac{1}{\sigma_{\theta k}}\mathrm{tr}\big(\tilde{\theta}_k^{\mathrm{T}}\dot{\hat{\theta}}_k\big) + \frac{b}{\varsigma} + c_{k-1}\end{aligned} \tag{29}$$

where $\theta_k \equiv [\bar{b}_k I_n, \bar{h}_k I_n, \bar{a}_1 I_n, \bar{b}_1 I_n, \bar{h}_1 I_n, \ldots, \bar{a}_{k-1}I_n, \bar{b}_{k-1}I_n, \bar{h}_{k-1}I_n]$, $\psi_k \equiv \big[\frac{z_k f_k^{\mathrm{T}}f_k}{\sqrt{z_k^{\mathrm{T}}z_k f_k^{\mathrm{T}}f_k + \epsilon_k^2}}; \frac{z_k\|\bar{x}_k\|^2}{\sqrt{z_k^{\mathrm{T}}z_k\|\bar{x}_k\|^2 + \epsilon_k^2}}; \frac{z_k\|\frac{\partial\bar{\upsilon}_{k-1}}{\partial x_1}\|^2\|\bar{x}_2\|^2}{\sqrt{z_k^{\mathrm{T}}z_k\|\frac{\partial\bar{\upsilon}_{k-1}}{\partial x_1}\|^2\|\bar{x}_2\|^2 + \epsilon_1^2}}; \frac{z_k\|\frac{\partial\bar{\upsilon}_{k-1}}{\partial x_1}\|^2 f_1^{\mathrm{T}}f_1}{\sqrt{z_k^{\mathrm{T}}z_k\|\frac{\partial\bar{\upsilon}_{k-1}}{\partial x_1}\|^2 f_1^{\mathrm{T}}f_1 + \epsilon_1^2}}; \frac{z_k\|\frac{\partial\bar{\upsilon}_{k-1}}{\partial x_1}\|^2\|\bar{x}_1\|^2}{\sqrt{z_k^{\mathrm{T}}z_k\|\frac{\partial\bar{\upsilon}_{k-1}}{\partial x_1}\|^2\|\bar{x}_1\|^2 + \epsilon_1^2}}; \ldots; \frac{z_k\|\frac{\partial\bar{\upsilon}_{k-1}}{\partial x_{k-1}}\|^2 x_k^{\mathrm{T}}x_k}{\sqrt{z_k^{\mathrm{T}}z_k\|\frac{\partial\bar{\upsilon}_{k-1}}{\partial x_{k-1}}\|^2 x_k^{\mathrm{T}}x_k + \epsilon_{k-1}^2}} + \frac{\kappa_k^2 z_{k-1}^{\mathrm{T}}z_{k-1}z_k}{\sqrt{\kappa_k^2 z_{k-1}^{\mathrm{T}}z_{k-1}z_k^{\mathrm{T}}z_k + \epsilon_{k-1}^2}}; \frac{z_k\|\frac{\partial\bar{\upsilon}_{k-1}}{\partial x_{k-1}}\|^2 f_{k-1}^{\mathrm{T}}f_{k-1}}{\sqrt{z_k^{\mathrm{T}}z_k\|\frac{\partial\bar{\upsilon}_{k-1}}{\partial x_{k-1}}\|^2 f_{k-1}^{\mathrm{T}}f_{k-1} + \epsilon_{k-1}^2}}; \frac{z_k\|\frac{\partial\bar{\upsilon}_{k-1}}{\partial x_{k-1}}\|^2\|\bar{x}_{k-1}\|^2}{\sqrt{z_k^{\mathrm{T}}z_k\|\frac{\partial\bar{\upsilon}_{k-1}}{\partial x_{k-1}}\|^2\|\bar{x}_{k-1}\|^2 + \epsilon_{k-1}^2}}\big]$, and κ_k is defined as

$$\kappa_k = \begin{cases}\xi_1, & k = 2 \\ 1, & 2 < k \leq n-1.\end{cases} \tag{30}$$

The auxiliary stabilizing function, $\bar{\upsilon}_k$, is then designed as

$$\bar{\upsilon}_k = -\frac{\hat{a}_k^2\upsilon_k^{\mathrm{T}}\upsilon_k z_k}{\sqrt{\hat{a}_k^2\upsilon_k^{\mathrm{T}}\upsilon_k z_k^{\mathrm{T}}z_k + \epsilon_k^2}}, \tag{31}$$

$$\upsilon_k = \hat{\theta}_k\psi_k - \varpi_k + \frac{1}{2}\rho z_k + \rho^2\frac{z_k}{z_k^{\mathrm{T}}z_k}, \tag{32}$$

where $\hat{a}_k$ and $\hat{a}_k$ are regulated by $\dot{\hat{a}}_k = \sigma_{ak}z_k^{\mathrm{T}}\upsilon_k - \rho\hat{a}_k$ and $\dot{\hat{\theta}}_k = \sigma_{\theta k}z_k\psi_k^{\mathrm{T}} - \rho\hat{\theta}_k$, respectively. Therefore, we can obtain a compact form of $\dot{V}_k$ through further consolidation and simplification

$$\begin{aligned}\dot{V}_k \leq\ & -\rho V_1 + \frac{b}{\varsigma} + z_k^{\mathrm{T}}A_k z_{k+1} \\ & - \sum_{j=2}^{k}\rho\left(\frac{1}{2}z_j^{\mathrm{T}}z_j + \frac{\underline{a}_j}{2\sigma_{aj}}\tilde{a}_j^2 + \frac{1}{2\sigma_{\theta j}}\mathrm{tr}\big(\tilde{\theta}_j^{\mathrm{T}}\tilde{\theta}_j\big)\right) + c_k\end{aligned} \tag{33}$$

where $c_k = c_{k-1} + \sum_{j=1}^{k}\epsilon_j(\bar{b}_j + \bar{h}_j + \bar{a}_j) + \frac{a_k^2}{8\sigma_{ak}^2} + \frac{\mathrm{tr}(\theta_k^{\mathrm{T}}\theta_k)^2}{8\sigma_{\theta k}^2} + \sum_{j=1}^{k-1}\epsilon_j\bar{a}_j$ and Young's inequality is utilized.

Step n. Consider the Lyapunov candidate as $V_n = V_{n-1}+\frac{1}{2}z_n^{\mathrm{T}}z_n+\frac{\underline{a}_n^*}{2\sigma_{an}}(\tilde{a}_n^*)^2+\frac{1}{2\sigma_{\theta n}}\mathrm{tr}(\tilde{\theta}_n^{\mathrm{T}}\tilde{\theta}_n)$, where $\sigma_{an}, \sigma_{\theta n} \in \mathbb{R}_+$, $a_n^* = 1/\underline{a}_n^* = 1/\underline{a}_n\vartheta_1$. $\tilde{a}_n^* = \hat{a}_n^* - a_n^*$ with $\hat{a}_n^*$ being the estimate of a_n^*. Integrating (33) and $z_n = x_n - \bar{v}_{n-1}$, in which $\bar{v}_{n-1}$ can be obtained in (31) for *Step* $n-1$, the time-derivative of V_n follows by combining (8) and (12)

$$\begin{aligned}\dot{V}_n =&\dot{V}_{n-1} + z_n^{\mathrm{T}}\dot{x}_n - z_n^{\mathrm{T}}\dot{\bar{v}}_{n-1} + \frac{\underline{a}_n^*}{\sigma_{an}}\tilde{a}_n^*\dot{\hat{a}}_n^* + \frac{1}{\sigma_{\theta n}}\mathrm{tr}\big(\tilde{\theta}_n^{\mathrm{T}}\dot{\hat{\theta}}_n\big)\\ =&\dot{V}_{n-1} + z_{n-1}^{\mathrm{T}}A_{n-1}z_n + z_n^{\mathrm{T}}(A_n\vartheta_1\tau + A_n\vartheta_2 + B_n^{\mathrm{T}}f_n\\ &+ h_n - \varpi_n) + \frac{\underline{a}_n^*}{\sigma_{an}}\tilde{a}_n^*\dot{\hat{a}}_n^* + \frac{1}{\sigma_{\theta n}}\mathrm{tr}\big(\tilde{\theta}_n^{\mathrm{T}}\dot{\hat{\theta}}_n\big),\end{aligned} \tag{34}$$

in which $\varpi_n = \sum_{j=1}^{n-1}\frac{\partial\bar{v}_{n-1}}{\partial x_{1d}^{(j-1)}}x_{1d}^{(j)} + \frac{\partial\bar{v}_{n-1}}{\partial k_c^{(j-1)}}k_c^{(j)} + \frac{\partial\bar{v}_{n-1}}{\partial\hat{\theta}_j}\dot{\hat{\theta}}_j$ $\frac{\partial\bar{v}_{n-1}}{\partial\Delta k_c^{(j-1)}}\Delta k_c^{(j)} + \frac{\partial\bar{v}_{n-1}}{\partial\hat{a}_j}\dot{\hat{a}}_j$. It is noticed from (34) that

$$\begin{aligned}z_n^{\mathrm{T}}(A_n\vartheta_2 + h_n) \le& \bar{a}_n\bar{\vartheta}_2\frac{z_n^{\mathrm{T}}z_n}{\sqrt{z_n^{\mathrm{T}}z_n+\epsilon_n^2}} + \frac{\bar{h}_n z_n^{\mathrm{T}}z_n\left\|\bar{x}_n\right\|^2}{\sqrt{z_n^{\mathrm{T}}z_n\left\|\bar{x}_n\right\|^2+\epsilon_n^2}}\\ &+ \epsilon_n(\bar{a}_n\bar{\vartheta}_2 + \bar{h}_n).\end{aligned} \tag{35}$$

Similarly, we have $z_n^{\mathrm{T}}B_n^{\mathrm{T}}f_n \le \bar{b}_n\frac{z_n^{\mathrm{T}}z_nf_n^{\mathrm{T}}f_n}{\sqrt{z_n^{\mathrm{T}}z_nf_n^{\mathrm{T}}f_n+\epsilon_n^2}} + \epsilon_n\bar{b}_n$. Design the virtual control law τ as

$$\tau = -\frac{(\hat{a}_n^*)^2\upsilon_n^{\mathrm{T}}\upsilon_n z_n}{\sqrt{(\hat{a}_n^*)^2\upsilon_n^{\mathrm{T}}\upsilon_n z_n^{\mathrm{T}}z_n+\epsilon_n^2}}, \tag{36}$$

$$\upsilon_n = \hat{\theta}_n\psi_n - \varpi_n + \frac{1}{2}\rho z_n + \rho^2\frac{z_n}{z_n^{\mathrm{T}}z_n}, \tag{37}$$

where ψ_n and ϖ_n will be defined later. $\hat{a}_n^*$ and $\hat{\theta}_n$ are updated by

$$\dot{\hat{a}}_n^* = \sigma_{an}z_n^{\mathrm{T}}\upsilon_n - \rho\hat{a}_n^*; \quad \dot{\hat{\theta}}_n = \sigma_{\theta n}z_n\psi_n^{\mathrm{T}} - \rho\hat{\theta}_n. \tag{38}$$

The above procedure establishes the foundation for the following Theorem.

B. Stability Analysis

Theorem 2. For a class of nonlinear MIMO systems (8) that satisfy *Assumptions* 1-2, using the prescribed-time controller (36) triggered by time-varying event (9)-(10) together with adaptive scheme regulated by (38), then the PPTS of the closed-loop system is guaranteed while the output state satisfies prescribed asymmetric constraint.

Proof. Substituting (35)-(36) into (34) and further simplifying, we have

$$\begin{aligned}\dot{V}_n \le& -\dot{V}_{n-1} - \underline{a}_n^*\hat{a}_n^*z_n^{\mathrm{T}}\upsilon_n + \frac{\bar{a}_{n-1}z_{n-1}^{\mathrm{T}}z_{n-1}z_n^{\mathrm{T}}z_n}{\sqrt{z_{n-1}^{\mathrm{T}}z_{n-1}z_n^{\mathrm{T}}z_n+\epsilon_n^2}}\\ &+ \frac{\bar{a}_n\bar{\vartheta}_2z_n^{\mathrm{T}}z_n}{\sqrt{z_n^{\mathrm{T}}z_n+\epsilon_n^2}} + \frac{\bar{b}_nz_n^{\mathrm{T}}z_nf_n^{\mathrm{T}}f_n}{\sqrt{z_n^{\mathrm{T}}z_nf_n^{\mathrm{T}}f_n+\epsilon_n^2}} - z_n^{\mathrm{T}}\varpi_n\\ &+ \frac{\bar{h}_nz_n^{\mathrm{T}}z_n\left\|\bar{x}_n\right\|^2}{\sqrt{z_n^{\mathrm{T}}z_n\left\|\bar{x}_n\right\|^2+\epsilon_n^2}} + \frac{\underline{a}_n^*}{\sigma_{an}}\tilde{a}_n^*\dot{\hat{a}}_n^* + \frac{\mathrm{tr}\big(\tilde{\theta}_n^{\mathrm{T}}\dot{\hat{\theta}}_n\big)}{\sigma_{\theta n}} + c_n^*,\end{aligned} \tag{39}$$

where $c_n^* = c_{n-1} + \epsilon_n(\underline{a}_n^* + \bar{b}_n + \bar{a}_n\bar{\vartheta}_2 + \bar{h}_n + \bar{a}_{n-1})$. It can be further simplified by combining (37)-(38) into (39)

$$\begin{aligned}\dot{V}_n \le& -\rho V_1 + \frac{b}{\varsigma} - \sum_{j=2}^{n}\frac{1}{2}\rho z_j^{\mathrm{T}}z_j - \sum_{j=2}^{n-1}\frac{\underline{a}_j\rho}{2\sigma_{aj}}\tilde{a}_j^2\\ &- \frac{\underline{a}_n^*\rho}{2\sigma_{an}}(\tilde{a}_n^*)^2 - \sum_{j=2}^{n}\frac{\rho}{2\sigma_{\theta j}}\mathrm{tr}\big(\tilde{\theta}_j^{\mathrm{T}}\tilde{\theta}_j\big) + c_n,\end{aligned} \tag{40}$$

where $\theta_n = [\bar{b}_nI_n, \bar{h}_nI_n, \bar{a}_n\bar{\vartheta}_2I_n, \bar{a}_{n-1}I_n, \theta_{n-1}]$, $\psi_n = [\frac{z_nf_n^{\mathrm{T}}f_n}{\sqrt{z_n^{\mathrm{T}}z_nf_n^{\mathrm{T}}f_n+\epsilon_n^2}}; \frac{z_n\|\bar{x}_n\|^2}{\sqrt{z_n^{\mathrm{T}}z_n\|\bar{x}_n\|^2+\epsilon_n^2}}; \frac{z_n}{\sqrt{z_n^{\mathrm{T}}z_n+\epsilon_n^2}}; \frac{z_{n-1}^{\mathrm{T}}z_{n-1}z_n}{\sqrt{z_{n-1}^{\mathrm{T}}z_{n-1}z_n^{\mathrm{T}}z_n+\epsilon_n^2}}; \psi_{n-1}]$, and $c_n = c_n^* + \frac{(a_n^*)^2}{8\sigma_{an}^2} + \frac{\mathrm{tr}(\theta_n^{\mathrm{T}}\theta_n)^2}{8\sigma_{\theta n}^2}$. As a consequence, we obtain $\dot{V}_n \le -\rho V_n + \frac{b}{\varsigma} + c_n$, which indicates that the equilibrium of closed-loop system is PPTS on the basis of *Theorem 1*. The boundedness of V_n can be obtained, namely for $t \in [t_0, t_T]$,

$$\begin{aligned}V_n(t) \le& \varsigma(t)\mathrm{e}^{-a(t-t_0)}\frac{V_n(0)}{\varsigma(t_0)} + \mathrm{e}^{-a(t-t_T)}\frac{b}{\alpha}(\varsigma+1)\\ \le& \mathrm{e}^{-a(t-t_0)}V_n(0) + \mathrm{e}^{-a(t-t_T)}\frac{b}{\alpha}(\varsigma+1),\end{aligned} \tag{41}$$

Since $V_n \le \frac{b}{\alpha}$ for $t > t_T$, we have the boundedness characteristic of V_1 in an iterative way, which further implies the boundedness of V_E due to $V_E \le V_1$. Thus, one can deduce $\|e_1 + \Delta k_c\| < k_c$ leading to $\left|e_{1j} + \Delta k_{cj}\right| < k_c$, which is equivalent to $\underline{k}_{cj} < e_{1j} < \bar{k}_{cj}$ for $j = 1, 2, ..., n$, where e_{1j} and Δk_{cj} are the jth element of e_1 and Δk_c, respectively; $\bar{k}_{cj} = k_c - \Delta k_{cj}$; $\underline{k}_{cj} = -k_c - \Delta k_{cj}$. That completes the proof.

Remark 5: With the convergence process of system trajectory, the terms ς and z_k will approach zero leading to a potential singularity in υ_k. Thus, we utilize a damped reciprocal to replace terms in the denominator of ς and $z_k^{\mathrm{T}}z_k$, respectively. Specifically, $z_k/z_k^{\mathrm{T}}z_k$ is transformed into the damped reciprocal form $z_k/z_k^{\mathrm{T}}z_k + \iota_k^2$ in implementing the controller, where $\iota_k \in \mathbb{R}_+$ is a small threshold. In this way, we have $z_k/z_k^{\mathrm{T}}z_k + \iota_k^2 \approx z_k/\iota_k^2$ for $\|z_k\| \ll \iota_k$, which also applies to the term with ς as the denominator to avoid singularity.

Remark 6: For $\forall t \in [t_k, t_{k+1})$, one can obtain $\frac{d}{dt}\left|\tau_j(t) - u_j(t)\right| = \frac{d}{dt}((\tau_j(t) - u_j(t))(\tau_j(t) - u_j(t)))^{\frac{1}{2}} = \mathrm{sign}(\tau_j(t) - u_j(t))(\dot{\tau}_j(t) - \dot{u}_j(t)) \le \left|\dot{\tau}_j(t)\right|$. It follows from (36) that $\tau_j(t)$ is bounded and continuously differentiable such that $\left|\dot{\tau}_j(t)\right| \le \chi_j$. In view of the fact that $\tau_j(t_k) - u_j(t_k) = 0$ and $\lim_{t\to t_{k+1}}\tau_j(t) - u_j(t) = \varkappa_i$, there exists a positive scalar $t^\star$ such that $\{t_{k+1} - t_k\} \ge t^\star \ge \varkappa_j/\chi_j$. Hence Zeno behavior can be effectively eliminated in the proposed control scheme.

Remark 7: Compared to existing works that focused on addressing symmetric constraints [41]–[43], we propose a novel unified control method based on bias state transformation to satisfy asymmetric constraint requirements. To achieve the prescribed asymmetric constraint $\underline{k}_{cj} < e_{1j} < \bar{k}_{cj}$ for $j = 1, 2, ..., n$, in which $\bar{k}_{cj} \in \mathbb{R}_+$ and $\underline{k}_{cj} \in \mathbb{R}_-$ are user-defined constraint functions, then k_c and Δk_c can be calculated as $k_c = \max\{k_{cj}\}$ and $\Delta k_c = \mathrm{col}\{\Delta k_{cj}\}$, where $k_{cj} = \bar{k}_{cj} - \underline{k}_{cj}/2$ and $\Delta k_{cj} = -\bar{k}_{cj} - \underline{k}_{cj}/2$, respectively. In particular, the bias constraint function becomes zero in the case of symmetric constraints, namely $\Delta k_{cj} = 0$. This approach transforms an asymmetric constraint into a symmetric one by means of bias state transformation, eliminating the need for a real-time determination of the sign of the constraint state or its associated state transformed variables, which thus avoids the singularity problem that may arise from the derivation of the sign function. As a consequence, the proposed control scheme is unified to address nonlinear MIMO systems with symmetric or asymmetric time-varying constraints.

IV. Simulation and Experiment

We carried out simulations and an experiment in two scenarios, namely *planar robot tracking* and *bimanual-local-single-remote tele-operation*, respectively, to test the proposed controller (36).

A. Simulation on 2-DoF Planar Robot

The plant considered in this simulation is a 2-DoF planar serial robot with dynamics

$$M(x_1)\dot{x}_2 + C(x_1, x_2)x_2 + G(x_1) + f(t) = u(t) \tag{42}$$

where x_1 and x_2 denote the joint angle and angular velocity, respectively. $M(x_1) = \begin{bmatrix} M_{11} & M_{12} \\ M_{21} & M_{22} \end{bmatrix}$ is the inertia matrix with $M_{11} = l_1^2(m_1 + m_2) + l_2^2 m_2 + 2l_1 l_2 m_2 \cos(x_{12})$, $M_{12} = M_{21} = l_2^2 m_2 + l_1 l_2 m_2 \cos(x_{12})$, $M_{22} = l_2^2 m_2$. x_{1j} and x_{2j} are the j-th element of x_1 and x_2 for $j = \{1, 2\}$. $C(x_1, x_2) = \begin{bmatrix} C_{11} & C_{12} \\ C_{21} & 0 \end{bmatrix}$ is the Coriolis and centrifugal force matrix, $C_{11} = -l_1 l_2 m_2 \sin(x_{12}) x_{22}$, $C_{12} = -l_1 l_2 m_2 \sin(x_{12})(x_{21} + x_{22})$, and $C_{21} = l_1 l_2 m_2 \sin(x_{12}) x_{21}$. $G(x_1) = [G_1, G_2]^{\mathrm{T}}$ is the gravity torque with $G_1 = (m_1 + m_2) l_1 g \cos(x_{11}) + m_2 l_2 g \cos(x_{11} + x_{12})$ and $G_2 = m_2 l_2 g \cos(x_{11} + x_{12})$. $f(t)$ is the lumped external disturbance and $u(t)$ is the control torque. The system parameters are set as $m_1 = m_2 = 2$kg, $l_1 = l_2 = 2$m, $g = 9.8$N/kg and $f = [10\sin(8t) + \bar{\omega}_1, 10\sin(10t) + \bar{\omega}_2]^{\mathrm{T}}$Nm with $\bar{\omega}_1$ and $\bar{\omega}_2$ being the random disturbance subject to $N(5, 10)$. The desired trajectory is set as $x_{1d} = [3\sin(2t + \frac{\pi}{2}) - 2, 2\sin(2t + \frac{\pi}{2}) - 1.2]^{\mathrm{T}}$rad. The initial condition is given by $x_1(0) = [3, -2]^{\mathrm{T}}$rad and $x_2(0) = [1, -1]^{\mathrm{T}}$rad/s. The control parameters are set as $a = 5$, $b = 10^{-4}$, $\beta_1 = \beta_2 = 0.4$, $\gamma_1 = \gamma_2 = 50$, $\alpha = 0.25$, $\epsilon = 1$, $\epsilon_1 = 10^{-5}$, $\sigma_{a1} = 0.5$, $\sigma_{\theta 1} = 3$, $\iota_1 = 0.05$. Exponential decay functions are chosen as $k_c = 4.6\exp(-4.5t) + 10^{-4}$ and $\Delta k_c = 0.4\exp(-4.5t) + 10^{-4}$ as in [44].

Simulation is performed with $T = 0.6$s, 1s and 1.5s. According to *Theorem 1*, the position synchronization errors need to reach $\|e_1\| \leq \sqrt{2b/\alpha} = 0.028$ when arriving at the pre-assigned settling time. Table I summarizes the transient and steady-state accuracy under the three parameters. We see that the output state can meet the specified accuracy at the specified time and rapidly reach a high convergence accuracy. Since the predetermined accuracy is greater than the value of the constraint function in the case of $T = 1.5$s, e_1 follows the constraint function in preference. In the other two cases, $\|e_1\|_{t=T}$ is basically equal, which indicates that the convergence time and accuracy are decoupled. Fig. 1 demonstrates the convergent profiles of the tracking errors, where $e_1 = x_1 - x_{1d}$, $e_2 = x_2 - \dot{x}_{1d}$, e_{j1} and e_{j2} are denoted as the first and second elements of e_j $(j = 1, 2)$, respectively. We see that the PPTS characteristic is guaranteed while the tracking error never violates the asymmetric constraints. Fig. 2 depicts the trigger moment and the released intervals of the controller under the action of the event trigger mechanism (9)-(10) in the case of $T = 0.6$s. During the transient-state process, the proposed controller takes only 0.166s to update and act on the driving joints, effectively reducing the computational burden.

We perform comparative simulations of finite-time control method with prescribed performance [6]. The control parameters are set to $T = 1$s with the initial value $x_1(0) = [2, -1]^{\mathrm{T}}$rad. The asymmetry of the constraint function is further enhanced by $k_c = 3.6\exp(-4.7t) + 10^{-4}$ and $\Delta k_c = 0.5\exp(-4t) + 10^{-4}$. The rest of the parameters are the same as in the simulation above. To ensure a fair comparison, we guarantee a settling time ($T = 1$s) driven by finite-time control [6] through the following parameters: $K_1 = K_2 = 2$, $\alpha_1 = \alpha_2 = 5$, $\gamma_1 = 4$, $\gamma_2 = 5/7$, $\mu = 0.001$, $\rho = 9/11$. Figs. 3(a) and (b) show that the proposed method overcomes the overshoot caused by the asymmetric constraints while achieving PPTS convergence. The singularity problem that often occurs in finite/fixed time control has also been effectively circumvented through employing damped reciprocal approach, as shown in Fig. 3(b). Compared with Fig. 1, it can be observed that the settling time in the proposed method is independent of the initial value and state constraints, but only determined by the time parameter T, thus validating the superiority of the proposed controller.

TABLE I
ACCURACY AT PREDETERMINED SETTLING TIME AND STEADY-STATE PROCESS.

	$\|e_1\|_{t=T}$	$\|e_1\|_{t=T+1\mathrm{s}}$	$\|e_2\|_{t=T}$	$\|e_2\|_{t=T+1\mathrm{s}}$
$T = 0.6$s	0.025	1.84×10^{-5}	0.049	5.88×10^{-4}
$T = 1.0$s	0.024	1.93×10^{-5}	0.089	1.93×10^{-4}
$T = 1.5$s	0.005	2.86×10^{-5}	0.031	5.19×10^{-4}

B. Experiment on Heterogeneous Teleoperation System

In the experiment, we asked the human operator to draw a two-dimensional circle trajectory with 9cm radius at the local side using two hands simultaneously. The teleoperation setup is composed of local and remote sides via a communication channel, where the operator manipulates the end handles of two 7-DoF Omega 7 haptic devices (Force Dimension Inc., Switzerland) based on visual feedback, as shown in Fig. 4(a). The command signals given by their two hands are integrated utilizing a Kalman filter to attenuate noise in the hands motion. Data transfer between human and the remote robot is realised via TCP/IP protocol, where the control frequency and additional latency are 100Hz and 0.5s. Inspired by [45], latency is introduced to test the savings in communication resources and robustness against delay-induced perturbations. The control objective for the remote robot is to track the state signal sent from the human operator. A 2-DoF simulated SCARA Robot is used as the remote site. Considering the workspace limitation, the exponential-decay constraint functions are set as $k_c = 4\exp(-4.6t) + 10^{-3}$ and $\Delta k_c = 0.1\exp(-4.6t) + 10^{-3}$. The desired joint positions sent from the local site are mapped from Cartesian space to joint one using inverse kinematics. It can be observed in Fig. 4(b) that the position tracking errors converge within the prescribed settling time and never exceed the user-defined asymmetric time-varying constraints. In addition, the velocity tracking performance is guaranteed as shown in Fig. 4(c). The PPTS characteristic is therefore ensured (i.e., $\|e_1\| \leq 9.38 \times 10^{-4}$(rad), $\|e_2\| \leq 5.5 \times 10^{-3}$(rad/s), $t > 1$s).

V. CONCLUSION

This paper introduced a new sufficient condition for *practically prescribed time stability* of nonlinear continuous-time systems. Based on piecewise scalar function, we propose a new adaptive event-triggered control scheme that ensures the tracking error converges to a prescribed convergence domain within a user-defined settling time. In addition, the EBLF-based control framework can effectively handle asymmetric output constraints with the help of bias state transformation, ensuring that the output state never violates the predefined constraints. This approach can deal with symmetrical and asymmetrical constraints in a unified PPTS control structure with a low computational burden, as a result of setting the bias constraint function. Therefore, critical performance metrics can be arbitrarily prescribed based on task requirements, including the settling time, convergence accuracy, and motion constraint, which provides a quantitative basis for parameter regulation.

REFERENCES

[1] S. P. Bhat and D. S. Bernstein, "Finite-time stability of continuous autonomous systems," *SIAM J. Control Optim.*, vol. 38, no. 3, pp. 751–766, Feb. 2000.
[2] S. P. Bhat and D. S. Bernstein, "Continuous finite-time stabilization of the translational and rotational double integrators," *IEEE Trans. Autom. Control*, vol. 43, no. 5, pp. 678–682, 1998.
[3] F. Amato, M. Ariola, and C. Cosentino, "Finite-time control of discrete-time linear systems: analysis and design conditions," *Automatica*, vol. 46, no. 5, pp. 919–924, 2010.

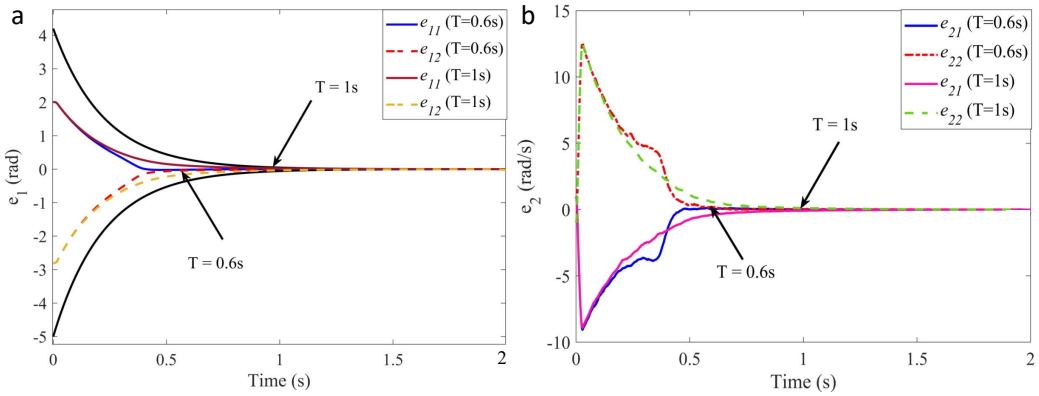

Fig. 1. Convergence profiles of tracking errors with the proposed controller (36). (a) Position tracking error. (b) Velocity tracking error (The black solid lines represent the asymmetric upper and lower constraints).

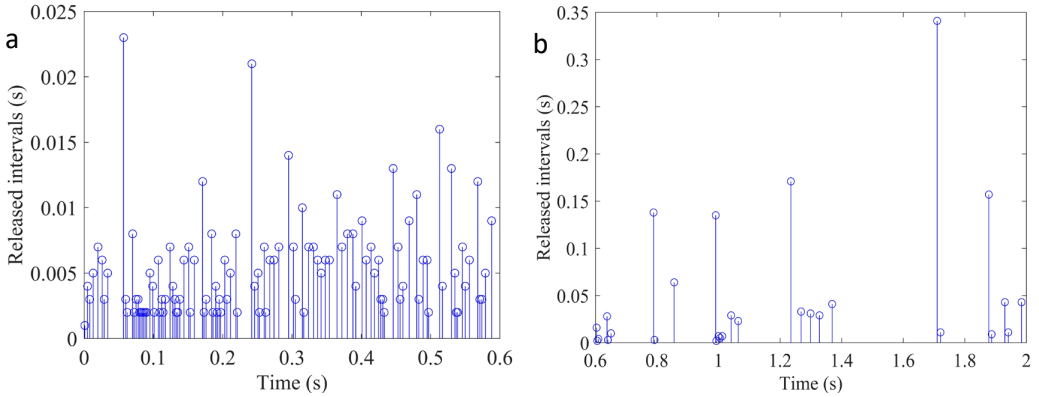

Fig. 2. Interval of triggering events under the controller (36) ($\boldsymbol{T = 0.6s}$). (a) Released intervals in transient-state process. (b) Released intervals in steady-state process.

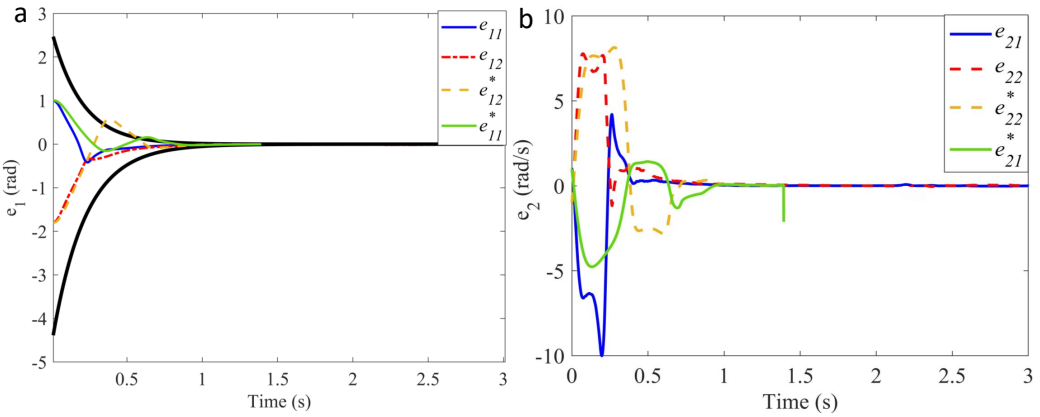

Fig. 3. Convergence profiles of tracking errors compared with [6]. (a) Position tracking errors. (b) Velocity tracking errors. (The black solid lines represent the asymmetric upper and lower constraint; * is with respect to finite-time control [6]).

[4] H. Ren, G. Zong, and T. Li, "Event-triggered finite-time control for networked switched linear systems with asynchronous switching," *IEEE Trans. Syst., Man, Cybern., Syst.*, vol. 48, no. 11, pp. 1874–1884, 2018.

[5] F. Wang, B. Chen, Y. Sun, Y. Gao, and C. Lin, "Finite-time fuzzy control of stochastic nonlinear systems," *IEEE Trans. Cybern.*, vol. 50, no. 6, pp. 2617–2626, 2020.

[6] Y. Yang, C. Hua, and X. Guan, "Finite time control design for bilateral teleoperation system with position synchronization error constrained," *IEEE Trans. Cybern.*, vol. 46, no. 3, pp. 609–619, 2016.

[7] S. Yu, X. Yu, B. Shirinzadeh, and Z. Man, "Continuous finite-time control for robotic manipulators with terminal sliding mode," *Automatica*, vol. 41, no. 11, pp. 1957 – 1964, 2005.

[8] Y. Feng, X. Yu, and Z. Man, "Non-singular terminal sliding mode control of rigid manipulators," *Automatica*, vol. 38, no. 12, pp. 2159–2167, 2002.

[9] Z. Zheng, Y. Xia, and M. Fu, "Attitude stabilization of rigid spacecraft with finite-time convergence," *Int. J. Robust Nonlinear Control.*, vol. 21, no. 6, pp. 686–702, 2011.

[10] Y. Shen and X. Xia, "Semi-global finite-time observers for nonlinear systems," *Automatica*, vol. 44, no. 12, pp. 3152 – 3156, 2008.

[11] A. Polyakov, "Nonlinear feedback design for fixed-time stabilization of linear control systems," *IEEE Trans. Autom. Control*, vol. 57, no. 8, pp. 2106–2110, Aug 2012.

[12] X. Jin, "Adaptive fixed-time control for MIMO nonlinear systems with asymmetric output constraints using universal barrier functions," *IEEE*

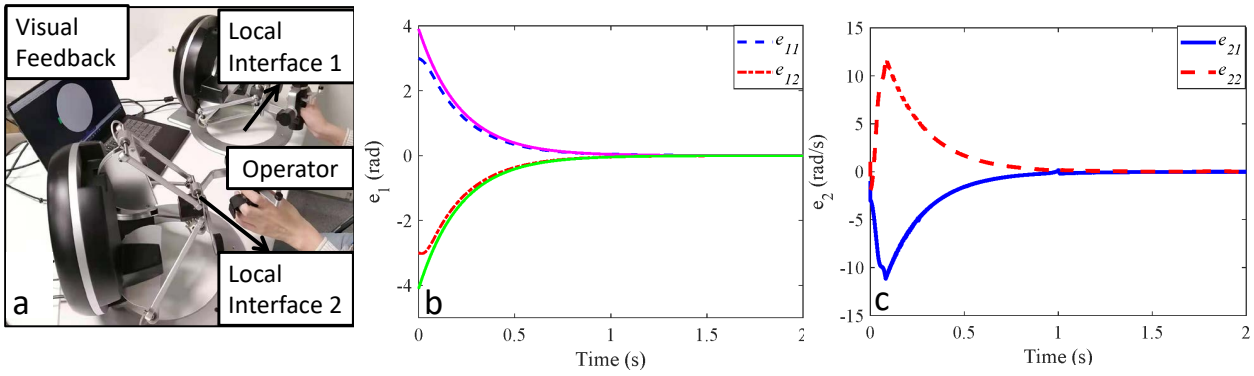

Fig. 4. Experimental Results in teleoperation. (a) Local experiment setup. (b,c) Tracking errors of the remote joint states.

Trans. Autom. Control, vol. 64, no. 7, pp. 3046–3053, 2019.

[13] Z. Wang, Z. Chen, Y. Zhang, X. Yu, X. Wang, and B. Liang, "Adaptive finite-time control for bilateral teleoperation systems with jittering time delays," *Int. J. Robust Nonlinear Control.*, vol. 29, no. 4, pp. 1007–1030, 2019.

[14] A. Polyakov, D. Efimov, and W. Perruquetti, "Finite-time and fixed-time stabilization: Implicit Lyapunov function approach," *Automatica*, vol. 51, pp. 332–340, 2015.

[15] B. Tian, Z. Zuo, X. Yan, and H. Wang, "A fixed-time output feedback control scheme for double integrator systems," *Automatica*, vol. 80, pp. 17–24, 2017.

[16] J. D. Sánchez-Torres, E. N. Sánchez, and A. G. Loukianov, "Predefined-time stability of dynamical systems with sliding modes," *2015 American Control Conference (ACC)*, pp. 5842–5846, 2015.

[17] E. Jiménez-Rodríguez, J. D. Sánchez-Torres, D. Gómez-Gutiérrez, and A. G. Loukianov, "Predefined-time stabilization of high order systems," in *2017 American Control Conference (ACC)*, 2017, pp. 5836–5841.

[18] Z. Kan, T. Yucelen, E. Doucette, and E. Pasiliao, "A finite-time consensus framework over time-varying graph topologies with temporal constraints," *J. Dyn. Sys., Meas., Control.*, vol. 139, no. 7, 05 2017.

[19] T. Yucelen, Z. Kan, and E. Pasiliao, "Finite-time cooperative engagement," *IEEE Trans. Autom. Control*, vol. 64, no. 8, pp. 3521–3526, 2019.

[20] Y. Song, Y. Wang, and M. Krstic, "Time-varying feedback for stabilization in prescribed finite time," *Int. J. Robust Nonlinear Control.*, vol. 29, no. 3, pp. 618–633, 2019.

[21] Y. Song, Y. Wang, J. Holloway, and M. Krstic, "Time-varying feedback for regulation of normal-form nonlinear systems in prescribed finite time," *Automatica*, vol. 83, pp. 243–251, 2017.

[22] P. Krishnamurthy, F. Khorrami, and M. Krstic, "Prescribed-time stabilization of nonlinear strict-feedback-like systems," in *2019 American Control Conference (ACC)*, 2019, pp. 3081–3086.

[23] P. Krishnamurthy, F. Khorrami, and M. Krstic, "Robust output-feedback prescribed-time stabilization of a class of nonlinear strict-feedback-like systems," in *2019 18th European Control Conference (ECC)*, 2019, pp. 1148–1153.

[24] D. V. Dimarogonas, E. Frazzoli, and K. H. Johansson, "Distributed event-triggered control for multi-agent systems," *IEEE Trans. Autom. Control*, vol. 57, no. 5, pp. 1291–1297, 2012.

[25] L. Ding, Q.-L. Han, X. Ge, and X.-M. Zhang, "An overview of recent advances in event-triggered consensus of multiagent systems," *IEEE Trans. Cybern.*, vol. 48, no. 4, pp. 1110–1123, 2018.

[26] W. Bai, T. Li, Y. Long, and C. L. P. Chen, "Event-triggered multigradient recursive reinforcement learning tracking control for multiagent systems," *IEEE Trans. Neural Netw. Learn. Syst.*, pp. 1–14, 2021.

[27] X. Liu, X. Su, P. Shi, C. Shen, and Y. Peng, "Event-triggered sliding mode control of nonlinear dynamic systems," *Automatica*, vol. 112, p. 108738, 2020.

[28] H. Li, Y. Wu, M. Chen, and R. Lu, "Adaptive multigradient recursive reinforcement learning event-triggered tracking control for multiagent systems," *IEEE Trans. Neural Netw. Learn. Syst.*, pp. 1–13, 2021.

[29] X. Chen, H. Yu, and F. Hao, "Prescribed-time event-triggered bipartite consensus of multiagent systems," *IEEE Trans. Cybern.*, pp. 1–10, 2020.

[30] K. P. Tee, S. S. Ge, and E. H. Tay, "Barrier Lyapunov functions for the control of output-constrained nonlinear systems," *Automatica*, vol. 45, no. 4, pp. 918–927, 2009.

[31] J.-X. Xu and X. Jin, "State-constrained iterative learning control for a class of MIMO systems," *IEEE Trans. Autom. Control*, vol. 58, no. 5, pp. 1322–1327, 2012.

[32] T. Gao, Y.-J. Liu, D. Li, S. Tong, and T. Li, "Adaptive neural control using tangent time-varying BLFs for a class of uncertain stochastic nonlinear systems with full state constraints," *IEEE Trans. Cybern.*, vol. 51, no. 4, pp. 1943–1953, 2021.

[33] Z. Wang, B. Liang, Y. Sun, and T. Zhang, "Adaptive fault-tolerant prescribed-time control for teleoperation systems with position error constraints," *IEEE Trans. Ind. Informat.*, vol. 16, no. 7, pp. 4889–4899, 2020.

[34] Z. Wang, H. Lam, B. Xiao, Z. Chen, B. Liang, and T. Zhang, "Event-triggered prescribed-time fuzzy control for space teleoperation systems subject to multiple constraints and uncertainties," *IEEE Trans. Fuzzy Syst.*, vol. 29, no. 9, pp. 2785–2797, 2021.

[35] B. Yang, W. Xiao, H. Yin, Q. Zhou, and R. Lu, "Adaptive neural control for multiagent systems with asymmetric time-varying state constraints and input saturation," *Int. J. Robust Nonlinear Control.*, vol. 30, no. 12, pp. 4764–4778, 2020.

[36] W. He, Z. Yin, and C. Sun, "Adaptive neural network control of a marine vessel with constraints using the asymmetric barrier Lyapunov function," *IEEE Trans. Cybern.*, vol. 47, no. 7, pp. 1641–1651, 2017.

[37] Z. Zheng, Y. Huang, L. Xie, and B. Zhu, "Adaptive trajectory tracking control of a fully actuated surface vessel with asymmetrically constrained input and output," *IEEE Trans. Control Syst. Technol.*, vol. 26, no. 5, pp. 1851–1859, 2018.

[38] J. Hale and S. M. V. Lunel, *Introduction to Functional Differential Equations*. Berlin: Springer, 1993.

[39] X. Jin, "Adaptive finite-time fault-tolerant tracking control for a class of MIMO nonlinear systems with output constraints," *Int. J. Robust Nonlinear Control.*, vol. 27, no. 5, pp. 722–741, 2017.

[40] L. Xing, C. Wen, Z. Liu, H. Su, and J. Cai, "Event-triggered adaptive control for a class of uncertain nonlinear systems," *IEEE Trans. Autom. Control*, vol. 62, no. 4, pp. 2071–2076, 2017.

[41] T. Gao, T. Li, Y.-J. Liu, and S. Tong, "IBLF-based adaptive neural control of state-constrained uncertain stochastic nonlinear systems," *IEEE Trans. Neural Netw. Learn. Syst.*, pp. 1–12, 2021.

[42] L. Cao, Q. Zhou, G. Dong, and H. Li, "Observer-based adaptive event-triggered control for nonstrict-feedback nonlinear systems with output constraint and actuator failures," *IEEE Trans. Syst., Man, Cybern., Syst.*, vol. 51, no. 3, pp. 1380–1391, 2021.

[43] Y. Cao, J. Cao, and Y. Song, "Practical prescribed time tracking control over infinite time interval involving mismatched uncertainties and non-vanishing disturbances," *Automatica*, vol. 136, p. 110050, 2022.

[44] J. Zhang and G. Yang, "Prescribed performance fault-tolerant control of uncertain nonlinear systems with unknown control directions," *IEEE Trans. Autom. Control*, vol. 62, no. 12, pp. 6529–6535, 2017.

[45] Y. Guo, D. Freer, F. Deligianni, and G.-Z. Yang, "Eye-tracking for performance evaluation and workload estimation in space telerobotic training," *IEEE Trans. Human-Mach. Syst.*, vol. 52, no. 1, pp. 1–11, 2022.